Available online at www.sciencedirect.com
ScienceDirect
Geochimica et Cosmochimica Acta 74 (2010) 5785–5797
Geochimica et Cosmochimica Acta
www.elsevier.com/locate/gca

Effects of aridity and vegetation on plant-wax δD in modern lake sediments

Pratigya J. Polissar *, Katherine H. Freeman

Department of Geosciences, The Pennsylvania State University, University Park, PA 16802, USA

Received 8 October 2009; accepted in revised form 8 June 2010; available online 25 June 2010

Abstract

We analyzed the deuterium composition of individual plant-waxes in lake sediments from 28 watersheds that span a range of precipitation D/H, vegetation types and climates. The apparent isotopic fractionation (ε_a) between plant-wax *n*-alkanes and precipitation differs with watershed ecosystem type and structure, and decreases with increasing regional aridity as measured by enrichment of ^2H and ^{18}O associated with evaporation of lake waters. The most negative ε_a values represent signatures least affected by aridity; these values were $-125 \pm 5‰$ for tropical evergreen and dry forests, $-130‰$ for a temperate broadleaf forest, $-120 \pm 9‰$ for the high-altitude tropical *páramo* (herbs, shrubs and grasses), and $-98 \pm 6‰$ for North American montane gymnosperm forests. Minimum ε_a values reflect ecosystem-dependent differences in leaf water enrichment and soil evaporation. Slopes of lipid/lake water isotopic enrichments differ slightly with ecosystem structure (i.e. open shrublands versus forests) and overall are quite small (slopes = 0–2), indicating low sensitivity of lipid δD variations to aridity compared with coexisting lake waters. This finding provides an approach for reconstructing ancient precipitation signatures based on plant-wax δD measurements and independent proxies for lake water changes with regional aridity. To illustrate this approach, we employ paired plant-wax δD and carbonate-$\delta^{18}O$ measurements on lake sediments to estimate the isotopic composition of Miocene precipitation on the Tibetan plateau.

1. INTRODUCTION

Plant-waxes are preserved over geologic timescales, and are found in diverse ancient sediments and soils (e.g. Pagani et al., 1999; Freeman and Colarusso, 2001). Observations that these molecules have hydrogen isotopic signatures that can be systematically related to that of modern precipitation (Sauer et al., 2001; Sachse et al., 2006; Smith and Freeman, 2006) have in recent years fueled aspirations to reconstruct ancient precipitation δD values. However, molecular isotopic signatures also reflect climate and plant physiological factors, and until better understood, these limit our ability to quantitatively interpret sedimentary lipid records. To advance our understanding of the influence of both ecosystem flora and climate (especially aridity) at the field scale, we analyzed the deuterium content of plant-waxes from sediments in 28 modern lakes located in watersheds which receive precipitation with a wide range of δD values, and are characterized by distinct vegetation types and regional climates.

1.1. Competing influences on plant-wax δD values

Evaporative influence on soil waters decreases with depth, with water near the soil surface most isotopically enriched (Barnes and Allison, 1988); plant water signatures will therefore reflect the depth(s) at which roots access soil water (e.g. Chimner and Cooper, 2004). Plants take up soil water without significant isotopic fractionation and, generally, water in plant stems reflects the isotopic composition of their soil water source (Ehleringer and Dawson, 1992). Stem water flows into leaves where

* Corresponding author. Present address: Division of Biology and Paleo Environment, Lamont-Doherty Research Institute of Columbia University, 61 Route 9W, Palisades, NY 10964, USA. Tel.: +1 845 365 8400; fax: +1 845 365 8150.
E-mail address: polissar@ldeo.columbia.edu (P.J. Polissar).

0016-7037/$ - see front matter © 2010 Elsevier Ltd. All rights reserved.
doi:10.1016/j.gca.2010.06.018

transpiration (evaporation from leaf stomata) enriches it in D and ^{18}O (e.g. Shu et al., 2008), with the magnitude intimately dependent upon leaf structure, transpiration rates and climate (Kahmen et al., 2008). Plant water signatures are transferred to plant-wax hydrogen with a negative offset due to biochemical fractionation (Sessions, 2006; Smith and Freeman, 2006; Hou et al., 2008).

n-Alkyl lipids can incorporate hydrogen from a number of preexisting biochemical compounds which also derive their hydrogen ultimately from plant water. These biochemicals are synthetic products from an earlier time, and thus their hydrogen isotope abundances can reflect climatic influences or precipitation isotopic signatures different than the leaf water at the time of lipid synthesis (Sessions, 2006). Processing of these biochemicals within the plant may also change their isotopic composition (Yakir, 1992). It is not well understood the degree to which variations in these hydrogen sources influence δD values of plant-waxes independent of any factors previously mentioned (Sessions et al., 1999; Sessions, 2006).

In contrast to the complex factors outlined above, datasets spanning large isotopic gradients in source water consistently find that precipitation δD values are the fundamental control on plant-wax compositions (e.g. Sauer et al., 2001; Sachse et al., 2004, 2006; Smith and Freeman, 2006; Hou et al., 2008; Liu and Yang, 2008). Further, simple models of soil evaporation capture much of the climate-dependent variation in datasets of plant-wax δD values (e.g. Smith and Freeman, 2006). Nevertheless, three key uncertainties remain. How do climate-driven changes in soil evaporation and plant transpiration influence lipid signatures? What is the role of vegetation type on the influences of leaf water enrichment, biosynthetic pools and the absorption of water from different soil pools? What is the combined influence of climate and vegetation for a natural ecosystem? A number of studies have examined these effects using individual plants (Sessions et al., 1999; Chikaraishi and Naraoka, 2003; Bi et al., 2005; Liu et al., 2006; Sachse et al., 2006, 2009; Sessions, 2006; Smith and Freeman, 2006; Hou et al., 2007). The sedimentary record integrates inputs from many vegetation sources, but few studies have addressed how climate and physiology affect the hydrogen isotopic signatures of plant-waxes from an assemblage of plant types at the scale of lake catchments.

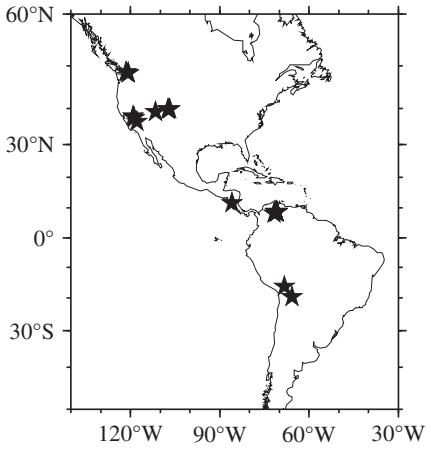

Fig. 1. Location of modern sediment samples.

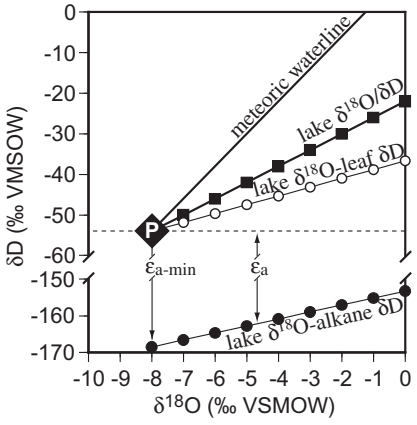

Fig. 2. Conceptual relationship between the $\delta^{18}O$ and δD of precipitation (large filled diamond), lake water (small filled squares), *n*-alkane δD and precipitation δD calculated from *n*-alkane δD. Filled circles plot lake water $\delta^{18}O$ versus *n*-alkane δD (lake–alkane evap.) assuming ε_a varies with $\varepsilon_{LW/ppt}$ based upon observations in this study (exhibited by the vertical separation between filled circles and horizontal dashed line). Open circles describe a lake–leaf evaporation line determined by lake water $\delta^{18}O$ values and precipitation δD values reconstructed from *n*-alkane δD values using a constant minimum apparent fractionation ($\varepsilon_{a\text{-}min}$).

1.2. Research approach

We sampled the surface sediments of lakes from North and South America (Fig. 1) representing a range of plant communities, climates and precipitation isotopic compositions, with the aim of testing the importance of these variables on measured plant-wax δD values. Sediment samples integrate input from vegetation sources throughout each lake's watershed and represent multiple years of accumulation. Accordingly, each sample records characteristics of the watershed ecosystem and integrates properties over time in a manner directly analogous to ancient sediments. We measured δD values of long-chain, odd-numbered *n*-alkanes extracted from these sediments and use previously reported lake water δD signatures (waters and sediments were collected at the same time).

Soil, leaf and lake waters acquire an isotopic signature from precipitation, and for all of these water types, enrichment with evaporation is governed by the same climate parameters (Fig. 2). Coupled isotope values for lake waters and plant-waxes should therefore co-evolve with evaporation, with the least-altered values providing the best proxy for the isotopic composition of precipitation. We develop this approach with modern samples and illustrate its application using measurements of lake calcite $\delta^{18}O$ and plant-wax δD values on Miocene lake sediments from Tibet.

2. MATERIALS AND METHODS

2.1. Sampling methods and sites

Surface lake sediments and watershed soils from Venezuela, Bolivia, Nicaragua, and the USA (Fig. 1) were collected using an Ekman sediment sampler, a sediment corer designed to collect an undisturbed sediment-water interface, or by hand (Table 1). The top one or two centimeters of Ekman samples were transferred to polyethylene vials or Whirl-Pak® sample bags. Surface sediment cores were extruded and sectioned in the field at 0.5–1.0 cm increments and transferred to Whirl-Pak® sample bags. Samples collected by hand were transferred to pre-combusted glass jars. Water samples from lakes, streams and springs were collected in Nalgene® polyethylene bottles by rinsing three times with sample water and then filling and capping the bottle underwater to remove any trapped air.

Vegetation at the Bolivian sites is dominated by *puna* grasslands (bunchgrass, herbs, moss, and lichens) with minor coverage from wetland plants along lake shorelines. The high-altitude sites in Venezuela encompass the unique alpine *páramo* vegetation (tussock grasses, ground rosettes, dwarf shrubs cushion plants, and conspicuous giant rosettes) while the lower elevation sites are covered with tropical cloud and evergreen forests. The Nicaraguan site, located on Isla Zapatera, is covered by dense tropical dry forest. Oak and laurel dominate the upland watershed around Bear Meadow in Pennsylvania, USA with pine, hemlock and maple in the proximal lowland bog forest. The North American montane forest sites in Colorado, Utah, Washington and California, USA vary from dense to patchy gymnosperm forests with variable angiosperm understory and meadow flora.

2.2. Measurement of water $\delta^{18}O$ and δD

Lake water isotope compositions come from samples collected to calibrate lake sediment-based paleoclimate reconstructions (Abbott et al., 2003; Polissar, 2005; Anderson and Rosenbaum, 2007) and published data (Payne and Yurtsever, 1974; White et al., 1990; Li et al., 1997; Ryu et al., 2002; O'Driscoll et al., 2005; Turich, 2006).

2.3. Extraction and purification of lipids

2.3.1. Solvent extraction

Freeze-dried sediments were extracted with a Dionex Accelerated Solvent Extraction (ASE) system. Two to 50 g of dried sediment were placed in the stainless-steel sample holders and extracted at 100 °C and 1000 psi with 10% (v/v) methanol/dichloromethane with a total volume of ~50 mL. These total lipid extracts (TLEs) were evaporated to near dryness with N_2 in a Turbovap solvent evaporator and transferred to 4 mL borosilicate vials with Teflon-lined caps. All remaining solvent was then evaporated and the TLE stored in a few drops of hexane at 4 °C.

2.3.2. Silica gel column chromatography

TLEs were separated into aliphatic (F1), ketone/alcohol/acid (F2), and polar (F3) fractions with silica gel column chromatography. Empty solid phase extraction columns with polyethylene frits (Varian Bond-Elute p/n 12131009 and 12131021) were rinsed with 8 mL each methanol, dicholoromethane and hexane. Silica gel (2.0 g Aldrich, 70–230 mesh, 60 Å; solvent extracted, activated 2 h at 200 °C and stored in a desiccator) was transferred in hexane to the SPE column and the column then rinsed twice with 6 mL hexane. The TLE was loaded on the column in 100 μL hexane and the F1, F2, and F3 fractions eluted with 5 mL of 10% dichloromethane in hexane, 8 mL ethyl acetate, and 5 mL methanol.

2.3.3. Saturated/unsaturated separation with Ag–silica gel chromatography

Aliphatic compounds (F1) were separated on 0.5 g Ag–silica gel in a Pasteur pipette. Saturated compounds were eluted with 4.5 mL hexane, and unsaturated compounds were eluted with 4.5 mL of 5% (v/v) ethyl acetate in hexane. Silver-impregnated silica gel was prepared by dissolving 3.0 g of silver nitrate in 75 mL of de-ionized water, adding 300 mL of methanol, and 60 g of silica gel and drying the mixture in a foil-covered rotary evaporator while gradually increasing the water temperature from 25 to 50 °C. The dry Ag–silica gel was heated at 120 °C for 16 h, capped and stored in a foil-covered desiccator.

2.3.4. Molecular sieve isolation of n-alkanes

Straight-chain *n*-alkanes were separated from branched/cyclic aliphatic compounds with a zeolite molecular sieve. The molsieve (type 5A, washed 40/60 mesh, Alltech Associates Inc., p/n 5602) was prepared by heating at 350 °C under vacuum ($<10^{-3}$ mb) for at least 12 h and stored in a desiccator.

Saturated aliphatic lipids and 0.5 g of activated molecular sieve were refluxed under N_2 in 3 mL *iso*-octane at 110 °C for 12 h. The supernatant was recovered and combined with seven hot *iso*-octane rinses of the molecular sieve to yield the branched/cyclic fraction. The *n*-alkyl lipids were recovered by transferring the dry molecular sieve to a 30 mL Teflon tube, adding 10 mL hexane followed by ~4 mL of 24% hydrofluoric acid (added dropwise with vigorous swirling) to dissolve the sieve and extracting the solution eight times with 5–10 mL aliquots of hexane. Tests with *n*-alkane standards demonstrated no hydrogen isotopic fractionation during the molsieve separation.

2.4. Lipid characterization by gas chromatography–mass spectrometry

Compounds were characterized by gas chromatography–mass spectrometry (GC–MS) using an Agilent 6890 GC with a split/splitless injector operated in splitless mode at 300 °C, a DB-5 column (0.25 mm i.d., 0.25 μm film thickness, 30 m length), 2.0 $cm^3\ min^{-1}$ He flow and programmed heating of the oven from 60 to 170 °C at 15 °C/min, and to 320 °C at 5 °C/min, and an Agilent 5973 quadrapole mass spectrometer. Compounds were identified by elution time, comparison with published spectra (Philp, 1985; Peters et al., 2004) and authentic standards.

2.5. Measurement of *n*-alkane δD

Compound-specific δD measurements were performed with an Agilent 6890 GC coupled via a high-temperature pyrolysis interface (Burgoyne and Hayes, 1998) and GCC III open split to a Finnegan Delta Plus XP isotope-ratio mass spectrometer equipped with an energy selective filter on the m/z 3 ion cup. Compounds were separated on a DB-5 column (0.25 mm i.d., 0.25 μm film thickness, 30 m length, 0.9 $cm^3\ min^{-1}$ He) and compound hydrogen quantitatively converted to H_2 in a high-purity alumina tube (0.5 mm i.d., 0.062 in. o.d., 30 mm length, Bolt Technical Ceramics) held at 1430 °C. Approximately 0.2 mL min^{-1} of the pyrolysis effluent was sent to the mass spectrometer via a 0.2 mm i.d. silica capillary. Every sample was co-injected with our laboratory standard (a mixture of *n*-C_{14} alkane, androstane, squalane and *n*-C_{41} alkane whose δD values were determined by Arndt Schimmelman, Indiana University via offline pyrolysis and dual-inlet analysis).

Table 1
Location, vegetation and water isotope compositions of study sites (data available as Electronic Annex EA-2).

Lake	Country	Longitude	Latitude	Elev. (m)	Vegetation	Lake (‰)				Precip. (‰)				Lake/ppt (‰)			
						$\delta^{18}O$	σ[a]	δD	σ[a]	$\delta^{18}O$	σ	δD	σ	ε^{18O}	σ	ε^{D}	σ
Laguna Potosi	Bol.	−65.69722	−19.63889	4640	*Puna* grassland	−5.6	0.6	−59	5	−11.9	1.5	−85	12[b]	6.4	1.7	29	15
Lago Taypi Chaka Kkota	Bol.	−68.35222	−16.20278	4300	*Puna* grassland	−14.9	0.6	−114	5	−16.1	1.3	−118	10[c]	—[f]		—[f]	
Laguna Arenales Alta	Ven.	−71.19418	8.72644	4005	Páramo shrubland	−9.6	0.6	−70	5	−10.7	1.9	−75	15[b]	1.1	2.0	6	17
Laguna Grande de los Patos	Ven.	−70.94877	8.81367	4190	Páramo shrubland	−1.2	1.3	−34	10	−12.7	0.5	−92	4[b]	11.7	1.4	64	12
Laguna La Cura	Ven.	−70.95292	8.81293	4230	Páramo shrubland	−7.0	0.6	−62	5	−12.3	0.6	−88	5[b]	5.3	0.9	29	8
Laguna Verdes Baja	Ven.	−70.87367	8.85813	4170	Superpáramo shrubland	−2.3	2.2	−40	13	−13.1	0.5	−95	4[b]	10.9	2.3	60	15
Laguna Verdes Medio	Ven.	−70.87353	8.85562	4192	Superpáramo shrubland	−1.9	1.5	−37	9	−13.1	0.5	−95	4[b]	11.4	1.6	63	11
Laguna Victoria	Ven.	−70.79995	8.81303	3211	Tropical cloud forest	−10.8	0.6	−75	5	−10.3	1.1	−72	9[b]	−0.5	1.3	−3	11
Laguna Negra	Ven.	−70.80502	8.78625	3460	Tropical cloud forest	−10.8	0.4	−74	4	−9.1	1.0	−63	8[b]	−1.7	1.1	−11	10
Laguna Mucubaji	Ven.	−70.82835	8.79658	3570	Páramo shrubland/pine forest	−10.0	0.5	−72	4	−10.8	1.1	−76	9[b]	0.7	1.2	5	10
Laguna Michurao Alto	Ven.	−70.86277	8.73038	3738	Páramo shrubland	−8.7	0.6	−66	5	−12.1	2.4	−87	19[b]	3.5	2.6	22	22
Laguna Misteque	Ven.	−70.88457	8.72013	3804	Páramo shrubland	−8.3	1.3	−64	10	−12.3	2.4	−89	19[b]	4.1	2.8	26	24
Laguna Royal "D"	Ven.	−70.87268	8.72827	3764	Páramo shrubland	−9.5	0.6	−72	5	−12.5	2.6	−90	21[b]	3.0	2.7	19	24
Laguna Royal "C"	Ven.	−70.87045	8.72180	3830	Páramo shrubland	−8.6	0.6	−66	5	−12.2	2.4	−87	19[b]	3.6	2.6	23	23
Laguna de La Pata	Ven.	−70.93402	8.65333	3980	Páramo shrubland	−6.6	1.3	−55	10	−12.5	2.3	−90	19[b]	6.0	2.7	39	24
Laguna Los Lirios	Ven.	−71.82657	8.30753	2305	Trop. evergreen broadleaf forest	−2.1	1.0	−23	8	−7.9	1.0	−53	8[b]	5.9	1.4	33	12
Laguna Zapatera	Nic.	−85.85000	11.76667	32	Trop. evergreen broadleaf forest	0.6	0.6	−8	5	−5.7	0.4	−39	0[b,d]	6.4	0.7	32	5
Berdeen Lake	USA, WA	−121.46708	48.71056	1561	Alpine gymno./angio. forest	−15.3	0.6	−107	5	−15.3	2.0	−107	16[b]	0.0	2.1	0	19
Rainy Lake	USA, WA	−120.73500	48.50333	1460	Alpine gymno./angio. forest	−17.2	0.6	−125	5	−17.2	1.2	−125	7[b]	0.0	1.4	0	10
Waddell Lake	USA, WA	−120.81650	48.43933	1500	Alpine gymno./angio. forest	−17.9	0.6	−128	5	−18.2	1.0	−131	8[c]	0.3	1.2	3	11
Owens Lake	USA, CA	−117.89217	36.49271	1147	Alpine forest, xerophytic shrub			−97	5	−15.0	2.0	−110	16[c,e]			15	19
Lake Crowley	USA, CA	−118.73920	37.58176	2058	Alpine forest, xerophytic shrub/gras					−17.4	1.0	−128	8[c]				
Mono Lake	USA, CA	−119.02741	37.94406	1899	Alpine forest, xerophytic shrub	−0.1	0.6		5	−13.8	1.0	−100	12[c]	13.8	1.2		
Blue (Eagle) Lake	USA, CO	−106.76401	39.75167	2536	Alpine gymno./angio. forest	−15.7	0.6	−117	5	−16.5	1.0	−122	8[e]	0.9	1.2	6	11
S. Grizzly Lake	USA, CO	−107.32514	39.69166	3239	Alpine gymno./angio. forest	−13.4	0.6	−101	4	−16.4	2.0	−118	16[e]	3.0	2.1	18	19
Bison Lake	USA, CO	−107.34623	39.76473	3276	Alpine gymno./angio. forest	−14.3	1.2	−108	7	−17.1	1.0	−123	8[e]	2.9	1.6	17	12
Emerald Lake	USA, UT	−111.49734	39.07426	3093	Alpine gymno./angio. forest	−11.6	0.7	−96	3	−15.7	2.1	−113	17[b]	4.2	2.2	19	20
Bear Meadows	USA, PA	−77.76217	40.72917	552	Oak forest	−9.9	0.6	−69	5	−9.9	1.9	−69	15[b,d]	0.0	2.0	0	17

[a] Uncertainty used for calculation of precipitation values (based upon range of values observed over time).
[b] Precipitation values determined from lake waters and a local evaporation line (see text). Uncertainty from propagated evaporation line and lake water uncertainties.
[c] Precipitation values determined from inflow stream.
[d] Precipitation values determined from precipitation.
[e] Precipitation values determined from groundwaters.
[f] Glacier meltwater increases lake water balance.

The contribution of H_3^+ to the m/z 3 ion beam was subtracted using a point-wise correction (Sessions et al., 2001) in the Isodat software package. The H_3^+ factor was measured daily with pulses of increasing reference gas amount. The m/z 2 and H_3^+-corrected m/z 3 traces were integrated in the Isodat software and the isotope ratio of individual peaks calculated relative to pulses of our laboratory reference H_2 gas introduced at the beginning and end of each GC run via the GCC III interface. The isotopic ratio of sample compounds on the VSMOW scale was calculated from these values using the co-injected squalane standard and long-term precision and accuracy was monitored with the co-injected androstane and n-C_{41} alkane standards. Over the course of 2 years, the 1σ of androstane and n-C_{41} δD was 3.9‰ and 2.8‰, respectively. All of our samples had peak areas larger than a minimum threshold below which δD values vary with peak area (~20 V-s for the PSU system, Polissar et al., 2009), and therefore were not corrected for peak size.

2.6. Precipitation $\delta^{18}O$ and δD values calculated from lakes and streams

Most of our study sites are located in remote alpine regions with little information on the isotopic composition of local precipitation. However, lake and stream waters reflect the isotopic composition of precipitation modified by evaporation, and it is possible to define the isotopic composition of precipitation from these waters if evaporative effects can be constrained.

Globally, the $\delta^{18}O$ and δD of precipitation are correlated, with a slope of ~8 and an intercept of +10‰ (Global Meteoric Water Line, GMWL, Rozanski et al., 1993). The slope of this line reflects near-equilibrium isotopic fractionation during vapor condensing to form precipitation, while the intercept is primarily determined by the extent of vapor recharge and humidity-controlled kinetic isotope effects during evaporation. Although local meteoric water lines (LMWL) may diverge from the GMWL for a variety of reasons, the available precipitation data for the regions in this study indicates that the local meteoric water lines are close to the GMWL (Payne and Yurtsever, 1974; Abbott et al., 2003; Polissar, 2005; I.A.E.A./W.M.O., 2006).

Evaporating water evolves towards more positive values along a $\delta^{18}O$–δD trajectory with a slope less than 8 (Fig. 2). This trajectory defines a local evaporation line (LEL) whose slope reflects kinetic isotope effects that largely depend upon the undersaturation of the atmosphere relative to the water surface and the isotopic composition of atmospheric moisture (Gonfiantini, 1986). Therefore the isotopic composition of evaporated lake or stream water is tied through the LEL to the unevaporated water source on the LMWL. This relationship provides a tool to estimate precipitation $\delta^{18}O$ or δD by 'projecting' evaporated lake or stream waters along a LEL to their intersection with the LMWL (Gibson et al., 2005). We take this approach, using the $\delta^{18}O$ and δD of lake and stream waters to develop local evaporation lines for each of the study regions and, by projecting to the local meteoric water line, we estimate precipitation $\delta^{18}O$ and δD values (details of this approach are available in Electronic Annex EA-1 and all water isotope data are available in Electronic Annex EA-4). Where available, published data on precipitation and meteoric-derived waters (Payne and Yurtsever, 1974; Ingraham and Taylor, 1991; Gonfiantini et al., 2001; O'Driscoll et al., 2005; Vimeux et al., 2005; Polissar et al., 2006) compare well to precipitation $\delta^{18}O$ and δD values determined from surface waters in our study (Electronic Annex EA-1).

Although estimated using LELs, all precipitation isotopic values are to a first order independent of the magnitude of lake evaporative enrichment. Local evaporation lines in each region were defined using two to six additional lakes near the sampled site, providing an independent constraint on evaporative trends and their extrapolation to precipitation values (data and results available in Electronic Annex EA-4). Also, lake values plot tightly along a local evaporation line and therefore any subset of individual values for a lake will define an identical precipitation isotopic composition that is independent of the extent of lake evolution along a LEL.

3. RESULTS AND DISCUSSION

3.1. *n*-Alkane abundance and δD

In all samples, the n-alkane distribution contains a long-chain maxima ($C_{27–33}$) with a pronounced odd-over-even preference (OEP). A second maxima with a strong OEP is sometimes present at mid-chain lengths ($C_{21–25}$), and a third maxima, consisting dominantly of C_{17}, is occasionally present. The chain lengths and OEP of these maxima correspond to the three common sources of organic matter in lacustrine settings: watershed vegetation, aquatic macrophytes and algae. Long-chain n-alkanes with a strong OEP are typical of epicuticular waxes from terrestrial plants (Eglinton and Hamilton, 1967), mid-length n-alkanes are commonly found in aquatic macrophyte vegetation (Ficken et al., 2000) and the C_{17} n-alkane is derived from algal sources within the lake itself. The abundance of these three maxima in any sample reflects the relative contributions of watershed vegetation, littoral aquatic plants and algae to the sedimentary organic matter.

Source inferences based on n-alkane chain length are corroborated by the high correlation between the δD values of C_{29} and C_{31} (likely both derived from plant leaf waxes, $r^2 = 0.88$, $n = 25$) and the lower correlations of these n-alkanes with mid- and short-chain homologues likely derived from aquatic macrophytes and algae (Tables 2 and 3). This grouping reflects a different δD value for each n-alkane source, determined by the physiology, environment and growth-water composition. For example, in dry regions evaporation from lakes is often greater than from soils, enriching the water used by algae and macrophytes for n-alkane synthesis and imprinting a more positive and variable δD signal in aquatic versus terrestrial plants (e.g. Mügler et al., 2008). This effect is illustrated by the generally more positive δD values of shorter-chain n-alkanes relative to the long-chain homologues in this dataset (Table 2).

The δD of precipitation has a wide range (−39‰ to −131‰) which fundamentally controls lake water δD values ($r^2 = 0.67$, $n = 28$) and broadly correlates with the δD of algal, macrophyte and terrestrial n-alkanes. The common influence of precipitation is illustrated by correlations (r^2) of 0.60 between C_{23} and C_{29} n-alkanes ($n = 15$) and 0.89 and 0.64 between the δD of C_{17} and that of the C_{23} ($n = 4$) and C_{29} n-alkanes ($n = 7$) (Table 3). The high correlation between all lake water values and estimated precipitation reflects the wide range of precipitation δD spanned by our entire dataset. This large range has a greater influence than evaporative effects at the watershed scale which act to decouple lake water isotope abundances from those of precipitation.

In the remainder of this paper, we focus on the δD of the C_{29} n-alkane as a representative measure of terrestrial

Table 2
Isotopic compositions of plant-wax *n*-alkanes. Replicate values were averaged prior to statistical analysis. An electronic version of this table is available as Electronic Annex EA-3.

Lake	Sample	*n*-Alkane δD (‰)														Alkane/ppt	
		C_{17}	σ	n	C_{23}	σ	n	C_{27}	σ	n	C_{29}	σ	n	C_{31}	σ	n	$\varepsilon_{C29/ppt}$	σ
Laguna Potosi	17–21 cm sed. depth[a]				−187		1	−184		1	−214		1	−202		1	−140	12[d]
Laguna Potosi	16–21 cm sed. depth[a]				−189		1	−184		1	−198		1	−198		1	−123	12[d]
Lago Taypi Chaka Kkota	Soil										−230	3	2	−232	3	2	−127	10
Lago Taypi Chaka Kkota	Sed.				−206		1	−215		1	−225		1	−232		1	−120	11[d]
Laguna Arenales Alta	Sed. R1[b]				−173		1	−190	3	3	−188	2	3	−199	1	3	−122	15
Laguna Arenales Alta	Sed. R2[b]										−184	2	2	−194	2	2	−117	15
Laguna Grande de los Patos	Sed.	−180		1	−145		1	−172		1	−191		1	−194		1	−109	6[d]
Laguna La Cura	Sed.	−181		1				−186		1	−187		1	−190		1	−108	6[d]
Laguna Verdes Baja	Sed., 5.5 m depth[c]										−187		1	−190		1	−102	6[d]
Laguna Verdes Baja	Sed., 4.0 m depth[c]							−171		1	−182		1	−185		1	−96	6[d]
Laguna Verdes Medio	Sed.										−180		1				−94	6[d]
Laguna Victoria	Sed.	−132	5	2				−191	1	2	−191	2	2	−198		2	−128	8
Laguna Negra (nr. Mucubaji)	Sed.							−182	2	2	−177	3	2	−192	2	2	−122	9
Laguna Mucubaji	Sed.										−192	2	3	−196	2	3	−126	9
Laguna Michurao Alto	Sed.										−188		1	−196		1	−110	19[d]
Laguna Misteque	Sed.							−193		1	−196		1	−198		1	−118	19[d]
Laguna Royal "D"	Sed.				−212		1	−202		1	−199		1	−198		1	−120	20[d]
Laguna Royal "C"	Sed.										−194		1	−201		1	−117	19[d]
Laguna de La Pata	Sed.										−189		1	−202		1	−108	19[d]
Laguna Los Lirios	Sed.	−133	5	2	−124	1	2	−156	2	2	−164	1	2	−174	1	2	−117	7
Laguna Zapatera	Sed.							−158		1	−159		1	−164		1	−125	4[d]
Berdeen Lake	Sed.							−206		1	−200	4	3	−200	3	3	−105	17
Rainy Lake	Sed.				−210		1				−210		1				−97	8[d]
Waddell Lake	Sed. R1[b]				−215	3	2	−226	2	2	−218	2	2	−210	2	2	−100	9
Waddell Lake	Sed. R2[b]										−215		1	−207		1	−96	10[d]
Owens Lake #1	Sed.	−230		1				−184		1	−191		1				−91	17[d]
Lake Crowley #1	Sed.	−261		1	−225	3	2	−241	2	2	−238	3	2	−225	2	2	−126	9
Mono Lake S. Tufa #1	Sed.				−173	1	2	−195	2	2	−194	1	2				−104	12
Blue (Eagle) Lake	Sed. R1[b]				−243		1	−233		1	−208		1	−212		1	−97	9[d]
Blue (Eagle) Lake	Sed. R2[b]	−240	3	2	−244	2	2	−237	1	2	−207	1	2	−206	1	2	−97	8
S. Grizzly Lake	Sed. R1[b]				−219	2	2	−223		2	−205	4	2	−205		1	−99	17
S. Grizzly Lake	Sed. R2[b]				−220		1	−222		1	−206		1	−204		1	−100	17[d]
Bison Lake	Sed. R1[b]				−214	5	3	−214	1	3	−205	3	3	−203	5	3	−93	9
Bison Lake	Sed. R2[b]				−213		1	−213		1	−206		1	−204		1	−94	9[d]
Emerald Lake	Sed.				−208	2	2	−212	0	2	−204	2	2	−200		2	−103	17
Bear Meadows	Sed.										−191		1				−131	15[d]

[a] Depth in sediment core (~1830–80 and 1830–90 A.D., Abbott and Wolfe, 2003).
[b] Replicate analyses (averaged for statistical treatment but shown individually in figures).
[c] Water depth.
[d] Analytical uncertainty of 4‰ used for calculation.

Table 3
Correlation coefficients (r^2) of δD values between *n*-alkane homologues and source waters (*n* ranges from 4 to 28, see Table 2).

	Ppt	LW	C_{17}	C_{23}	C_{27}	C_{29}	C_{31}
Ppt	1						
LW	0.67	1					
C_{17}	0.94	0.55	1				
C_{23}	0.69	0.77	0.89	1			
C_{27}	0.72	0.85	0.60	0.88	1		
C_{29}	0.7	0.71	0.64	0.60	0.78	1	
C_{31}	0.65	0.66	0.72	0.50	0.71	0.88	1

plant-wax δD. We choose C_{29} because it is abundant in both tree and grass plant-waxes and has the highest concentration of the long-chain *n*-alkanes in most of our samples. We found similar results with the δD of the C_{29} and C_{31} homologues, although C_{27} values potentially reflect small contributions from aquatic macrophytes (Table 3) (Ficken et al., 2000) that can have quite different δD values from terrestrial sources (Mügler et al., 2008). We chose to examine the δD of individual *n*-alkanes rather than a composite (such as the abundance-weighted mean) which could be affected by biosynthetic δD differences between homologues (cf. Chikaraishi et al., 2004) that could obscure environmental relationships.

3.2. Isotopic fractionation between *n*-alkane and precipitation

Following previous studies (Sauer et al., 2001) we calculate an apparent fractionation between the *n*-alkane and local precipitation:

$$\alpha_{\text{apparent}} = (\delta D_{C29} + 1)/(\delta D_{\text{precipitation}} + 1) \quad (1)$$

and express this fractionation using the epsilon notation in units of permil (‰):

$$\varepsilon_a = (\alpha_a - 1) \quad (2)$$

Apparent fractionation incorporates the effects of soil evaporation, transpiration and biosynthesis, and differences between sites and regions reflect differing plant physiology, ecosystem structure and aridity. In the following sections we examine these factors using samples representing a diversity of climates and ecosystem types.

3.2.1. Role of vegetation

There is a broad range of ε_a across all sites (Table 2), however, when samples are grouped by the dominant type of vegetation in each watershed, several patterns emerge (Figs. 3 and 4). Tropical forests (cloud, semi-evergreen and dry evergreen) have an average ε_a of -125 ± 4‰ ($\pm 1\sigma$), similar to the one sample from a mid-latitude oak-dominated forest (−131‰). In contrast, for gymnosperm-dominated mid-latitude alpine conifer forests and tundra, average $\varepsilon_a = -101 \pm 10$‰, significantly smaller than the angiosperm-dominated temperate and tropical forests. High-altitude tropical sites dominated by parámo vegetation have an average ε_a of -108 ± 9‰. Finally, the high-altitude *puna* grasslands of the Bolivian *altiplano* have an ε_a of -128 ± 6‰.

Plant functional type-dependent differences in leaf water enrichment may explain some of the patterns in ε_a we observe between ecosystems. For example, *puna* grasslands have an average ε_a that is about 19‰ lower than the *páramo* sites, possibly reflecting the dominance of C_3-monocot vegetation in the *altiplano puna* grasslands relative to the dominantly C_3-dicot angiosperms of the páramo. Greater apparent fractionation in monocot versus dicot angiosperms is also observed in greenhouse and field samples (Smith and Freeman, 2006, and references therein). The −126‰ ε_a of the *puna* grasslands is similar to that of grasses growing at highly arid sites in the US Great Plains (−127‰ to −147‰, Smith and Freeman, 2006), and much higher than values for grasses growing in humid Great Plains locations (∼−189, Smith and Freeman, 2006) consistent with evaporative enrichment in soil and plant waters of the extremely arid *altiplano*.

The similarity of ε_a in tropical dry evergreen and cloud forests of Venezuela (avg. -123 ± 5‰), the semi-evergreen tropical forest of Nicaragua (−125‰) and the temperate deciduous forest of Pennsylvania (−131‰) suggests little variation in the ε_a of C_3 angiosperm trees. This result compares well to studies of lake sediments from angiosperm tree-dominated watersheds in Europe (-133 ± 11, $n = 7$, Sachse et al., 2004). The similarity of ε_a across widely differing angiosperm tree communities and climates suggests plant-wax δD enrichments are relatively insensitive to local conditions, including climate.

The smallest ε_a values in this study were from gymnosperm-dominated alpine forests of the Rocky, Sierra Nevada, and Cascade Mountains. These values are smaller than either the páramo or angiosperm forest groups, a surprising result because previous studies have not found significant differences between angiosperm and gymnosperm plant lipids in natural settings. Intuitively, ε_a values of −101‰ suggest profound evapotranspiration effects compared to angiosperm trees. However, no systematic differences were observed between gymnosperm and angiosperm individuals grown in the same environment at a variety of Asian sites (Chikaraishi and Naraoka, 2003; Bi et al., 2005; Liu and Yang, 2008) or between plant lipids from gymnosperm- and angiosperm-dominated watersheds in Europe (Sachse et al., 2004). Alternatively, we suggest the answer lies in the seasonal isotopic differences in precipitation: for our gymnosperm-dominated alpine sites, winter and summer can differ by 160‰ δD (Ingraham and Taylor, 1991; Welker, 2000; Robertson and Gazis, 2006). The apparent fractionation for these samples is calculated from a precipitation value that averages winter and summer precipitation (Henderson and Shuman, 2009). If plants mostly use isotopically enriched summertime precipitation, then the true ε_a would be several tens permil lower than the value calculated using the annual average.

Enriched δD values of lipid precursors could also cause smaller ε_a values in our middle- and high-latitude gymnosperm-dominated catchments. Biosynthetic precursors of plant-wax *n*-alkanes, such as acetate contribute as much as 25% of the total H in *n*-alkanes (Sessions, 2006). The δD of acetate follows that of its sugar precursors, whether derived directly from photosynthesis (primary photosynthate)

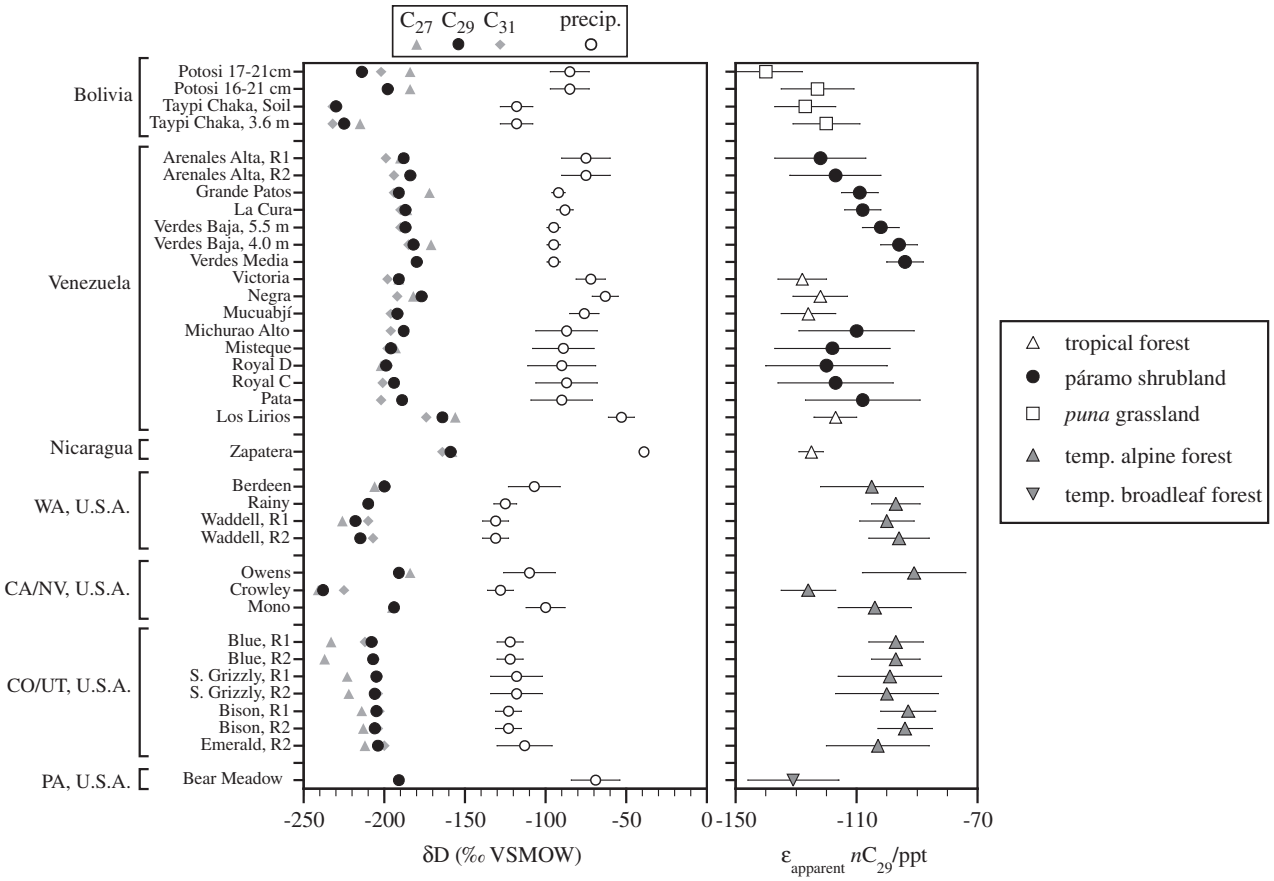

Fig. 3. Hydrogen isotopic composition of local precipitation and *n*-alkanes homologues (left panel) and the apparent fractionation between the C_{29} *n*-alkane and precipitation (right panel). The type of vegetation is indicated by the symbol pattern. Numbers after location names indicate different water depths in meters from the same lake or different core depths in centimeters, while R1 and R2 indicate analyses of two samples from the same lake and water depth. Horizontal lines are 1σ ranges.

or from stored carbohydrates (stored reserves, using the terminology of Roden et al., 2002). Primary photosynthate has a strongly negative δD signature that is reflected in carbohydrates immediately derived from this source (Yakir, 1992). However, the δD values of carbohydrates become more positive during heterotrophic reprocessing, therefore plants using significant stored reserves to synthesize plant-waxes may imprint a more positive δD and thus ε_a on the *n*-alkane molecules. Seasonal changes in the photosynthesis/respiration ratio, possibly driven by the large changes in temperature and daylight at middle- and high-latitude locations, could increase the amount of stored reserves used to synthesize *n*-alkanes. These *n*-alkanes would have an average δD more positive than those synthesized from primary photosynthate, perhaps providing an alternative (or additional) explanation for the small apparent fractionation values observed in the alpine gymnosperm flora.

Grouping apparent fractionation factors by ecosystem offers strong evidence that different plant assemblages fractionate plant-wax hydrogen isotopes to different degrees. Much of these differences could reflect the influence of leaf physiology on transpiration and leaf water isotopic enrichment. Ecosystem structure such as soil cover and shading likely also play an important role by affecting soil evaporation. Apparent fractionation measured using *n*-alkanes in lake sediments thus captures plant community differences in ecosystem structure and plant functional types; below we explore the climatic sensitivity of these differences.

3.2.2. *Aridity increases n-alkane δD and ε_a*

Evaporative enrichment of lakes—like water in plants and soil—is largely controlled by relative humidity and the amount of precipitation relative to evaporation. Indeed, isotope models for soil evaporation and plant transpiration are derived from the same equations governing the hydrologic and isotopic balance of lake systems (e.g. Gonfiantini, 1986; Barnes and Allison, 1988; Shu et al., 2008). The enrichment of lake water relative to precipitation ($\varepsilon_{LW/ppt}$) is a potentially useful measure of climatic effects on evaporative enrichment of waters in plants and soils and ultimately on plant-wax δD variations.

Aridity-induced lake water enrichment is anticipated to correlate with isotopic enrichments in leaf water, but the relationship is potentially complex. The water and isotopic balance of a lake is modified by the lake/watershed area ratio and catchment hypsometry while leaf water enrichment also depends upon transpiration rates and stomatal conductance. We note that many of our sites are

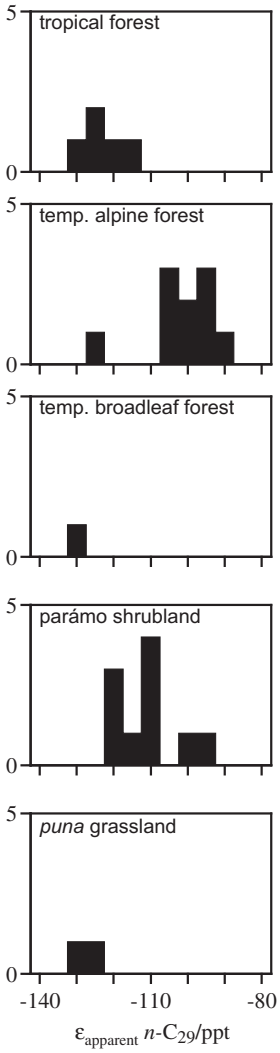

Fig. 4. Histograms illustrating the relationship between plant type and the apparent fractionation between the C_{29} *n*-alkane and local precipitation.

moraine-dammed lakes in glacial valleys with similar lake/watershed area ratios and elevation hypsometries (data available in Electronic Annex EA-2), tending to minimize effects from differences in these variables. A supplementary analysis of the relationship between lake water enrichment, lake/watershed areas and climate data (where available) is available in Electronic Annex EA-1. In this analysis we find that lake water enrichment is negatively correlated with the slope of the evaporation line indicating lower relative humidity at more enriched sites. We also find little relationship between evaporative enrichment and the watershed/lake area ratio suggesting climate—not catchment and lake size—is the primary determinant of enrichment. Limited climate data from tropical sites and more plentiful data from US locations supports these inferences (Electronic Annex EA-1). Five of the study lakes exhibit an exception to this pattern. All five are terminal lakes with large lake/watershed areas whose isotopic composition is at the maximum enrichment expected for a lake system where evaporation equals inflow. The evaporative enrichment of these lakes continues to be sensitive to relative humidity but should be insensitive to changes in the precipitation/evaporation ratio (Gonfiantini, 1986). We include these lakes in our analysis because their enrichment, while reflecting higher lake/watershed areas, also reflects drier conditions in these regions (Weingarten et al., 1991; Pulwarty et al., 1998). Their inclusion decreases the slope of any relationship between lake enrichment and plant-wax δD, yielding minimum estimates for the effect of climate on δD_{wax}. Finally, for the highly seasonal environments in this study, lake enrichment is a semi-quantitative gauge for the year-round evaporative enrichment within a watershed, however, plants may preferentially synthesize lipids during a specific growing season.

Examining variations of ε_a relative to the isotopic enrichment of lake water (Fig. 5) reveals that *páramo* samples plot along lines of increasing ε_a and $\varepsilon_{LW/ppt}$. The positive relationship indicates that *páramo* ecosystems, like lake evaporation, respond sympathetically to aridity. The spread of apparent fractionation values within the páramo vegetation type (Fig. 4) is therefore partly a result of climatic differences, and the range of ε_a values under similar climates is considerably smaller than the range of ε_a values across all sites. In contrast, ε_a in tree-dominated ecosystems shows little relationship to lake water enrichment.

3.2.3. Fundamental differences of ε_a between ecosystems

The average ε_a values from most studies of modern plant specimens are inherently biased by their sampling distribution which rarely captures relevant climate gradients. This potentially biases published values for plant types and can cause inappropriate application of ε_a values to ancient samples, as to do so assumes that past growth conditions were similar to the mean of the dataset used to determine average ε_a values. To circumvent this problem, we define ε_a values for our sampled ecosystems under a reference climate state provided by the $\varepsilon_{a\text{-min}}$, that is, when lake water evaporation is minimal ($\varepsilon_{LW/ppt} = 0$).

The intercept of the ε_a–$\varepsilon_{LW/ppt}$ relationships with the line of zero lake water enrichment ($\varepsilon_{LW/ppt} = 0$) in Fig. 5 allows us to compare $\varepsilon_{a\text{-min}}$ values between ecosystems when isotopic enrichment from soil and stomatal evaporation are minimized by the wettest recorded conditions for that setting. Values for minimum ε_a are -98 ± 6 for alpine forests, -120 ± 9 for páramo and -125 ± 5 for tropical broadleaf forests (Fig. 5 and Table 4).

3.2.4. Sensitivity of ε_a to climate

The slope of the ε_a–$\varepsilon_{LW/ppt}$ relationship provides a means to compare ε_a-climate relations for different ecosystems. Large values for the slope indicate a considerable influence of climate on soil and leaf evaporation while small values reflect negligible climatic influences. Included in this analysis are the effects of watershed vegetation on lake water balance. Water yield (precipitation minus evapotranspiration) is generally higher in grass versus tree-covered catchments due to lower rates of transpiration (Rosenmeier et al., 2002), therefore in equivalent climates, less isotopic enrichment of lake water will occur in grass

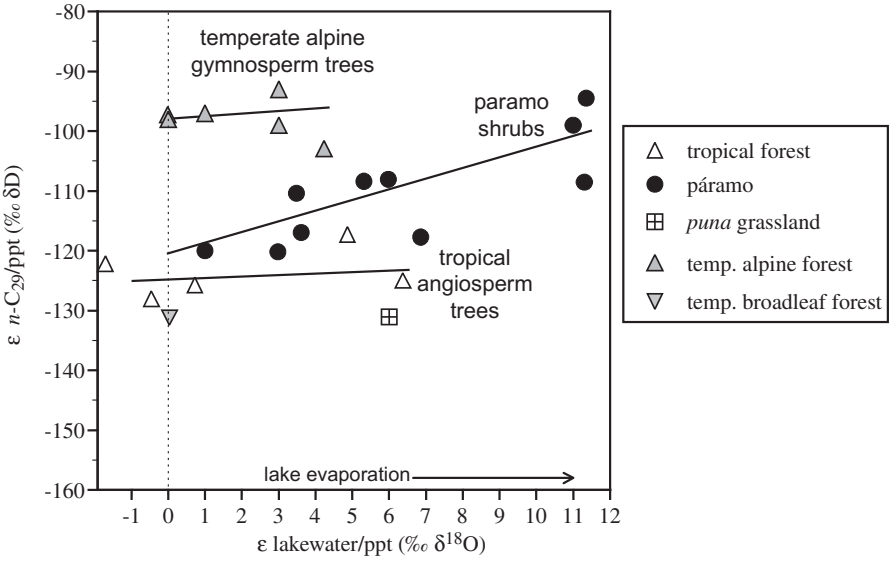

Fig. 5. Relationship between the isotopic enrichment of lake water from local precipitation and the apparent fractionation between the C_{29} *n*-alkane and local precipitation. Solid lines are linear regression fits to the data (Table 4). Vertical dashed line indicates zero lake water enrichment (negative values are within 1σ of zero, Table 1). Note that conifer values could be too high if these plants preferentially access growth season (summer) precipitation that is enriched relative to the average annual precipitation.

Table 4
Regression coefficients ($\pm 1\sigma$) of lake water $\delta^{18}O$ enrichment versus plant-wax δD enrichment in Fig. 5. Replicate measurements were averaged prior to regression and the regression includes both *x*- and *y*-value uncertainties (Press et al., 1994) that are assumed uncorrelated. Similar regression statistics with equal or smaller uncertainties were found when correlation of *x*- and *y*-uncertainties was included using a Monte Carlo approach (details presented in Electronic Annex EA-1).

Vegetation	Slope	Intercept	r^2
Tropical forest	0.2 ± 0.8	-125 ± 5	0.08
Temp. alpine forest	0.4 ± 2.3	-98 ± 6	0.89
Páramo shrubland	1.8 ± 0.9	-120 ± 9	0.64

versus tree-dominated systems (with intermediate values for shrubby ecosystems). This effect would decrease the slope of the relationship between leaf-wax δD and lake water enrichment in grass-dominated systems, with minimal effect on the minimum apparent fractionation values calculated above.

The ε_a–$\varepsilon_{LW/ppt}$ slope (using the $\delta^{18}O$ of lake waters) is 1.8 ± 0.9 ($\pm 1\sigma$) for the páramo, 0.4 ± 2.3 for the mid-latitude alpine forests and 0.2 ± 0.8 for tropical forests (Fig. 5 and Table 4). The slopes for forested catchments are near zero, showing little influence of climate on soil-leaf evaporation. The larger, positive slopes of the *páramo* vegetation samples suggest greater evaporative effects in these shrub- and grass-dominated ecosystems (e.g. Victoria et al., 1991; Tsujimura et al., 2007). A greater propensity for soil evaporation yields potentially stronger climate sensitivity in grass and shrubby ecosystems relative to transpiration-dominated water loss in canopied forests. Canopies decrease the absorption of sunlight by the soil and decouple the free atmosphere from the soil surface, reducing the energy and diffusion gradients necessary for soil evaporation. The low (to zero) slopes in all ecosystems may also be significantly influenced by the timing of plant-growth if leaf growth and *n*-alkane production is greater at times when stomatal and soil evaporation is less (such as rainy seasons or cooler times of the day).

3.3. Interpreting plant-wax δD in ancient samples

Our approach builds on that suggested by Sachse et al. (2004) for interpreting ancient *n*-alkane δD values in the context of source water (precipitation) and climate. First, paleoecology is constrained using pollen, leaf fossils or other paleobotanical indicators in order to define a minimum apparent fractionation factor ($\varepsilon_{a\text{-}min}$) based upon modern analogs of the ancient ecosystem and/or its plant functional types (Polissar et al., 2009). Next, paired plant-wax δD estimates of precipitation (using $\varepsilon_{a\text{-}min}$) and inferred isotopic compositions of lake water $\delta^{18}O$, such as that calculated from carbonates (using temperature-dependent fractionation factors) or from D/H of algal lipids (using published $\varepsilon_{W\text{-}L}$ data, Sachse et al., 2004; Zhang and Sachs, 2007; Mügler et al., 2008) are compared for each sample. The reconstructed leaf and lake water isotope values should plot on or to the right of the LMWL, depending upon the extent of evaporation. The isotopic composition of precipitation along the LMWL is tied to these $\delta^{18}O$–δD values through a lake/leaf water evaporation line (LLEL) whose trend is ~0–2, depending upon the type(s) of vegetation (Fig. 5). (Please note, this trend is slightly curved in $\delta^{18}O$–δD space and is described by a quadratic equation derived in Electronic Annex EA-1.) Projecting the evaporated water composition to the LMWL using paired lake/plant data yields an estimate for the composition of the precipitation source to the catchment.

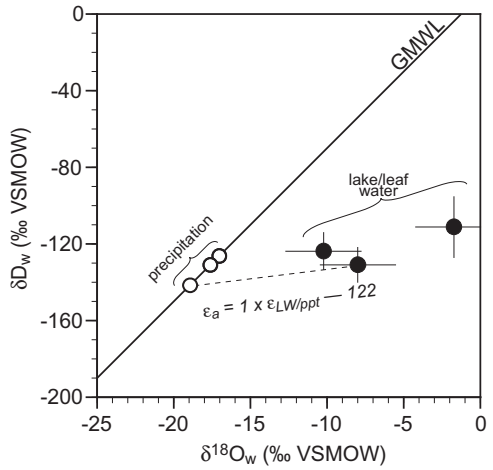

Fig. 6. Hydrogen and oxygen isotopic composition of evaporated waters and unevaporated precipitation calculated from plant-waxes and lacustrine carbonates of the Miocene Dinqing Formation (Lunpola Basin, Tibetan plateau, Rowley and Currie, 2006; Polissar et al., 2009). Water δD was calculated from plant-wax δD with an ε_a of $-121 \pm 10‰$ and water $\delta^{18}O$ was calculated from carbonate-$\delta^{18}O$ assuming equilibrium fractionation at 10 ± 10 °C (Friedman and O'Neil, 1977). Pollen analyses indicate ~1:1 gymnosperm:angiosperm sources for the plant-wax *n*-alkanes (Xia, 1983). Precipitation values were calculated from waters using the GMWL and a leaf water/lake water evaporation slope of 1.0‰ δD/‰ $\delta^{18}O$ (see text).

The utility of this approach is illustrated by paired lipid δD and carbonate-$\delta^{18}O$ measurements on Miocene lacustrine sediments from the Lunpola Basin, China (Fig. 6). The isotopic compositions of waters inferred from these measurements plot to the right of the meteoric water line, indicating enrichment from evaporation. Projection of these water compositions along a lake/leaf water evaporation trend of 1.0 (reflecting a mixed forest/shrubland) to the meteoric water line provides an estimate for the $\delta^{18}O$ and δD of Miocene precipitation at this location on the Tibetan plateau (Polissar et al., 2009). This result is noteworthy because the value of precipitation calculated with our approach is indistinguishable from the most negative $\delta^{18}O_w$ value inferred from carbonates at this locality, even though this negative value was not used for our calculation. The inference is that coupled plant-wax δD and carbonate-$\delta^{18}O$ values from a strongly evaporative system can reproduce the most negative $\delta^{18}O_w$ values that are presumably the least affected by evaporation and closest to the isotopic value of local precipitation. Future endeavors could focus on quantitative modeling of coupled lake water and plant-wax isotopic enrichments to quantitatively relate climate, vegetation and geographic factors to measured δD_{wax} and $\delta^{18}O_{CaCO3}$ values.

4. FUTURE DIRECTIONS

Sorting out the importance of soil evaporation, stomatal evaporation, and biosynthetic processes in determining the δD values of plant molecules remains a persistent goal in modern studies. The challenge for ancient studies represented by this knowledge gap is illustrated by the small apparent fractionations we observed in alpine gymnosperm forests, which could equally be explained by greater summer versus winter precipitation sources, large evaporation effects, small biosynthetic fractionations or variable precursors to *n*-alkane biosynthesis. Future studies that include isotopic measurements on water and biosynthetic precursors to *n*-alkane synthesis (e.g. precipitation, soil, stem and leaf water, primary photosynthate, stored reserves, acetate) and are carried out under large climate gradients would provide a means to evaluate the climate sensitivity of individual processes that control ε_a in individual plants. In contrast, the work presented here is carried out at the ecosystem and catchment scale to understand how plant type, ecosystem structure (through its effects on surface-atmosphere fluxes of energy and water) and climate (especially aridity) can combine to affect plant-wax δD. Ultimately, we hope better understanding of isotope signatures at the plant scale will enable theoretical estimates for ε_a in different vegetation assemblages and settings, and yield a deterministic model for comparison of plant-wax and environmental data in modern and ancient lake catchments.

5. CONCLUSION

We determined the apparent fractionation of hydrogen isotopes between sedimentary plant-wax *n*-alkanes and local precipitation for lakes representing a variety of vegetation groups and climates. We examined how apparent fractionation changes with increasing aridity (inferred from the isotopic enrichment of lake water due to evaporation) and in dissimilar ecosystems. These differences reflect the influence of plant physiology and the physical structure of ecosystems on isotopic effects during soil evaporation and transpiration. Biosynthetic differences are potentially important, but cannot be separately evaluated from our data. As isotopic enrichment of lake water increases, apparent fractionation for shrubs and grass-dominated ecosystems has a slightly positive slope, providing evidence that aridity affects plant-wax δD. The slope increase is negligible in tree-dominated watersheds suggesting that closed ecosystem structure can dampen the response of plant-wax δD to climate. For all ecosystems, changes in apparent fractionation with aridity are much less compared to equivalent lake water enrichments suggesting plant-wax δD values are a better recorder of precipitation δD than mineral or algal archives. Our findings emphasize that both climate and vegetation effects must be evaluated when interpreting plant-wax δD and we suggest an approach for interpreting plant-wax δD in ancient samples that include these effects to provide estimates for the isotopic composition of paleoprecipitation.

ACKNOWLEDGMENTS

This research was supported by a National Science Foundation grant to K.H.F. and P.J.P. (EAR-0741400) and post-doctoral funding for P.J.P. from the Canadian Institute for Advanced Research-Earth System Evolution Program. Thoughtful reviews from Sarah Feakins, Dirk Sachse and one anonymous reviewer helped to

improve the manuscript. We gratefully acknowledge sediment samples and water isotope data contributed by Lesleigh Anderson (U.S.G.S.), Mark Abbott (University of Pittsburgh) and Katherine Huntington (University of Washington). We thank Dennis Walizer and Nevin Whitman for analytical assistance.

APPENDIX A. SUPPLEMENTARY DATA

Supplementary data associated with this article can be found, in the online version, at doi:10.1016/j.gca.2010.06.018.

REFERENCES

Abbott M. B. and Wolfe A. P. (2003) Intensive pre-Incan metallurgy recorded by lake sediments from the Bolivian Andes. *Science* **301**, 1893–1895.

Abbott M. B., Wolfe B. B., Wolfe A. P., Seltzer G. O., Aravena R., Mark B. G., Polissar P. J., Rodbell D. T., Rowe H. D. and Vuille M. (2003) Holocene paleohydrology and glacial history of the central Andes using multiproxy lake sediment studies. *Palaeogeogr. Palaeoclimatol. Palaeoecol.* **194**, 123–138. doi:10.1016/S0031-0182(03)00274-8.

Anderson L. and Rosenbaum J. G. (2007) Holocene paleohydrology of the upper Colorado River from lake sediment studies on the White River Plateau, Colorado. *Geol. Soc. Am. Abstr. Programs* **39**(6), 431.

Barnes C. J. and Allison G. B. (1988) Tracing of water movement in the unsaturated zone using stable isotopes of hydrogen and oxygen. *J. Hydrol.* **100**(1–3), 143.

Bi X., Sheng G., Liu X., Li C. and Fu J. (2005) Molecular and carbon and hydrogen isotopic composition of n-alkanes in plant leaf waxes. *Org. Geochem.* **36**, 1405–1417.

Burgoyne T. W. and Hayes J. M. (1998) Quantitative production of H2 by pyrolysis of gas chromatographic effluents. *Anal. Chem.* **70**, 5136–5141.

Chikaraishi Y. and Naraoka H. (2003) Compound-specific dD–d13C analyses of *n*-alkanes extracted from terrestrial and aquatic plants. *Phytochemistry* **63**, 361–367.

Chikaraishi Y., Suziki Y. and Naraoka H. (2004) Hydrogen isotope fractionations during desaturation and elongation associated with polyunsaturated fatty acid biosynthesis in marine macroalgae. *Phytochemistry* **65**, 2293–2300.

Chimner R. A. and Cooper D. J. (2004) Using stable oxygen isotopes to quantify the water source used for transpiration by native shrubs in the San Luis Valley, Colorado, USA. *Plant Soil* **260**(1), 225.

Eglinton G. and Hamilton R. J. (1967) Leaf epicuticular waxes. *Science* **156**, 1322–1335.

Ehleringer J. R. and Dawson T. E. (1992) Water uptake by plants: perspectives from stable isotope composition. *Plant Cell Environ.* **15**(9), 1073–1082.

Ficken K. J., Li B., Swain D. L. and Eglinton G. (2000) An *n*-alkane proxy for the sedimentary input of submerged/floating freshwater aquatic macrophytes. *Org. Geochem.* **31**, 745–749.

Freeman K. H. and Colarusso L. A. (2001) Molecular and isotopic records of C4 grassland expansion in the late Miocene. *Geochim. Cosmochim. Acta* **65**(9), 1439–1454.

Friedman I. and O'Neil J. R. (1977) Compilation of stable isotopic fractionation factors of geochemical interest. In *Data of Geochemistry* (ed. M. Fleischer). U.S. Geological Survey Professional Paper 440-K, p. 12.

Gibson J. J., Edwards T. W. D., Birks S. J., St. Amour N. A., Buhay W. M., Mceachern P., Wolfe B. B. and Peters D. L. () Progress in isotope tracer hydrology in Canada. *Hydrol. Process.* **19**(1), 303–327.

Gonfiantini R. (1986) Environmental isotopes in lake studies. In *Handbook of Environmental Isotope Geochemistry*, vol. 2 (eds. P. Fritz and J. C. Fontes). Elsevier, pp. 113–168.

Gonfiantini R., Roche M.-A., Olivry J.-C., Fontes J.-C. and Zuppi G. M. (2001) The altitude effect on the isotopic composition of tropical rains. *Chem. Geol.* **181**, 147–167.

Henderson A. K. and Shuman B. N. (2009) Hydrogen and oxygen isotopic compositions of lake water in the western United States. *Geol. Soc. Am. Bull.* **121**(7–8), 1179–1189. doi:10.1130/B26441.1.

Hou J., D'andrea W. J., Macdonald D. and Huang Y. (2007) Hydrogen isotopic variability in leaf waxes among terrestrial and aquatic plants around Blood Pond, Massachusetts (USA). *Org. Geochem.* **38**, 977–984.

Hou J., D'andrea W. J. and Huang Y. (2008) Can sedimentary leaf waxes record D/H ratios of continental precipitation? Field, model, and experimental assessments. *Geochim. Cosmochim. Acta* **72**, 3503–3517.

I.A.E.A./W.M.O. (2006) Global Network of Isotopes in Precipitation. The GNIP Database. <http://isohis.iaea.org/> (accessed).

Ingraham N. L. and Taylor B. E. (1991) Light stable isotope systematics of large-scale hydrologic regimes in California and Nevada. *Water Resour. Res.* **27**(1), 77–90.

Kahmen A., Simonin K., Tu K. P., Merchant A., Callister A., Siegwolf R., Dawson T. E. and Arndt S. K. (2008) Effects of environmental parameters, leaf physiological properties and leaf water relations on leaf water d18O enrichment in different Eucalyptus species. *Plant Cell Environ*. doi:10.1111/j.1365-3040.2008.01784.x.

Li H.-C., Ku T.-L., Stott L. D. and Anderson R. F. (1997) Stable isotope studies of Mono Lake (California): 1. d18O in lake sediments as proxy for climatic change during the past 150 years. *Limnol. Oceanogr.* **42**(2), 230–238.

Liu W. and Yang H. (2008) Multiple controls for the variability of hydrogen isotopic compositions in higher plant n-alkanes from modern ecosystems. *Global Change Biol.* **14**(9), 2166–2177.

Liu W., Yang H. and Li L. (2006) Hydrogen isotopic compositions of n-alkanes from terrestrial plants correlate with their ecological life forms. *Oecologia* **150**, 330–338.

Mügler I., Sachse D., Werner M., Xu B., Wu G., Yao T. and Gleixner G. (2008) Effect of lake evaporation on dD values of lacustrine n-alkanes: a comparison of Nam Co (Tibetan Plateau) and Holzmaar (Germany). *Org. Geochem.* **39**(6), 711–729. doi:10.1016/j.orggeochem.2008.02.008.

O'Driscoll M. A., Dewalle D. R., Mcguire K. J. and Gburek W. J. (2005) Seasonal ^{18}O variations and groundwater recharge for three landscape types in central Pennsylvania, USA. *J. Hydrol.* **303**, 108–124.

Pagani M., Freeman K. H. and Arthur M. A. (1999) Isotope analyses of molecular and total organic carbon from Miocene sediments. *Geochim. Cosmochim. Acta* **64**(1), 37–49.

Payne B. R. and Yurtsever Y. (1974) Environmental isotopes as a hydrogeological tool in Nicaragua. In *Symposium on Isotope Techniques in Groundwater Hydrology*, pp. 193–202.

Peters K. E., Walters C. C. and Moldowan J. M. (2004) *The Biomarker Guide*. Cambridge University Press.

Philp R. P. (1985) *Fossil Fuel Biomarkers*. Elsevier Science Publishing Company Inc.

Polissar P. J. (2005) Lake records of Holocene climate change, Cordillera de Mérida, Venezuela. Ph.D. dissertation, University of Massachusetts.

Polissar P. J., Abbott M. B., Shemesh A., Wolfe A. P. and Bradley R. S. (2006) Hydrologic balance of tropical South America

from oxygen isotopes of lake sediment opal, Venezuelan Andes. *Earth Planet. Sci. Lett.* **242**, 375–389. doi:10.1016/j.epsl.2005.12.024.

Polissar P. J., Freeman K. H., Rowley D. B., Mcinerney F. A. and Currie B. S. (2009) Paleoaltimetry of the Tibetan Plateau from D/H ratios of lipid biomarkers. *Earth Planet. Sci. Lett.* **287**, 64–76. doi:10.1016/j.epsl.2009.07.037.

Press W. H., Teukolosky S. A., Vetterling W. T. and Flannery B. P. (1994) *Numerical Recipes in C*. Cambridge University Press.

Pulwarty R. S., Barry R. G., Hurst C. M., Sellinger K. and Mogollon L. F. (1998) Precipitation in the Venezuelan Andes in the context of regional climate. *Meteorol. Atmos. Phys.* **67**, 217–237.

Robertson J. A. and Gazis C. A. (2006) An oxygen isotope study of seasonal trends in soil water fluxes at two sites along a climate gradient in Washington State (USA). *J. Hydrol.* **328**(1–2), 375.

Roden J. S., Lin G. and Ehleringer J. R. (2002) Response to the comment of V.J. Terwilliger on "A mechanistic model for interpretation of hydrogen and oxygen isotope ratios in tree-ring cellulose," by J.S. Roden, G. Lin, and J.R. Ehleringer (2000) Geochim. Cosmochim. Acta 64:21–35. *Geochim. Cosmochim. Acta* **66**(4), 733–734.

Rosenmeier M. F., Hodell D. A., Brenner M., Curtis J. H. and Guilderson T. P. (2002) A 4000-year lacustrine record of environmental change in the southern Maya Lowlands, Petén, Guatemala. *Quatern. Res.* **57**(2). doi:10.1006/qres.2001.2305.

Rowley D. B. and Currie B. S. (2006) Palaeo-altimetry of the late Eocene to Miocene Lunpola basin, central Tibet. *Nature* **439**. doi:10.1038/nature04506.

Rozanski K., Araguás-Araguás L. and Gonfiantini R. (1993) Isotopic patterns in modern global precipitation. In *Climate Change in Continental Isotopic Records*, vol. 78 (eds. P. K. Swart, K. C. Lohmann, J. A. Mckenzie and S. M. Savin). American Geophysical Union, pp. 1–36.

Ryu J.-H., Gao S., Dahlgren R. A. and Zierenberg R. A. (2002) Arsenic distribution, speciation and solubility in shallow groundwater of Owens Dry Lake, California. *Geochim. Cosmochim. Acta* **66**(17), 2981–2994.

Sachse D., Kahmen A. and Gleixner G. (2009) Significant seasonal variation in the hydrogen isotopic composition of leaf-wax lipids for two deciduous tree ecosystems (*Fagus sylvativa* and *Acer pseudoplatanus*). *Org. Geochem.* **40**(6), 732.

Sachse D., Radke J. and Gleixner G. (2004) Hydrogen isotope ratios of recent lacustrine sedimentary n-alkanes record modern climate variability. *Geochim. Cosmochim. Acta* **68**(23), 4877–4889.

Sachse D., Radke J. and Gleixner G. (2006) DD values of individual n-alkanes from terrestrial plants along a climatic gradient—implications for the sedimentary biomarker record. *Org. Geochem.* **37**, 469–483.

Sauer P. E., Eglinton T. I., Hayes J. M., Schimmelmann A. and Sessions A. L. (2001) Compound specific D/H ratios of lipid biomarkers from sediments as a proxy for environmental and climatic conditions. *Geochim. Cosmochim. Acta* **65**(2), 213–222.

Sessions A. L. (2006) Seasonal changes in D/H fractionation accompanying lipid biosynthesis in *Spartina alterniflora*. *Geochim. Cosmochim. Acta* **70**, 2153–2162.

Sessions A. L., Burgoyne T. W. and Hayes J. M. (2001) Correction of H3+ contributions in hydrogen isotope ratio monitoring mass spectrometry. *Anal. Chem.* **73**(2), 192–199.

Sessions A. L., Burgoyne T. W., Schimmelmann A. and Hayes J. M. (1999) Fractionation of hydrogen isotopes in lipid biosynthesis. *Org. Geochem.* **30**, 1193–1200.

Shu Y., Feng X., Posmentier E. S., Sonder L. J., Faiia A. M. and Yakir D. (2008) Isotopic studies of leaf water: Part 1. A physically based two-dimensional model for pine needles. *Geochim. Cosmochim. Acta* **72**(21), 5175–5188. doi:10.1016/j.gca.2008.05.062.

Smith F. A. and Freeman K. H. (2006) Influence of physiology and climate on dD of leaf wax n-alkanes from C3 and C4 grasses. *Geochim. Cosmochim. Acta* **70**(5), 1172–1187.

Tsujimura M., Sasaki L., Yamanaka T., Sugimoto A., Li S.-G., Matsushima D., Kotani A. and Saandar M. (2007) Vertical distribution of stable isotopic composition in atmospheric water vapor and subsurface water in grassland and forest sites, eastern Mongolia. *J. Hydrol.* **333**(1), 35.

Turich C. H. (2006) Molecular and isotopic investigations of the biogeochemistry of archaeal ether lipids. Ph.D. dissertation, The Pennsylvania State University.

Victoria R. L., Martinelli L. A., Mortatti J. and Richey J. (1991) Mechanisms of water recycling in the Amazon Basin: isotopic insights. *Ambio* **20**(8), 384–387.

Vimeux F., Gallaire R., Bony S., Hoffman G. and Chiang J. C. H. (2005) What are the climate controls on dD in precipitation in the Zongo Valley (Bolivia)? Implications for the Illimani ice core interpretation. *Earth Planet. Sci. Lett.* **240**, 205–220.

Weingarten B., Salgado-Labouriau M. L., Yuretich R. and Bradley R. (1991) Late quaternary environmental history of the Venezuelan Andes. In *Late Quaternary Climatic Fluctuations of the Venezuelan Andes*, vol. 65 (ed. R. Yuretich). University of Massachusetts, pp. 63–94.

Welker J. M. (2000) Isotopic d18O characteristics of weekly precipitation collected across the USA: an initial analysis with application to water source studies. *Hydrol. Process.* **14**(8), 1449–1464.

White A. F., Peterson M. L., Wollenberg H. and Flexser S. (1990) Sources and fractionation processes influencing the isotopic distribution of H, O and C in the Long Valley hydrothermal system, California, USA. *Appl. Geochem.* **5**(5–6), 571.

Xia J.-B. (1983) Cenozoic of Baingoin and its borders, Xizang (Tibet). In *Contribution to the Geology of the Qinghai-Xizang (Tibet) Plateau*, vol. 3. Ministry of Geology and Mineral Resources, PRC, pp. 243–254.

Yakir D. (1992) Variations in the natural abundance of oxygen-18 and deuterium in plant carbohydrates. *Plant Cell Environ.* **15**, 1005–1020. doi:10.1111/j.1365-3040.1992.tb01652.x.

Zhang Z. and Sachs J. P. (2007) Hydrogen isotope fractionation in freshwater algae: I. Variations among lipids and species. *Org. Geochem.* **38**, 582–608.

Associate editor: Josef Werne